

Reaction rate uncertainties and ^{26}Al in AGB silicon carbide stardust

M. A. van Raai¹, M. Lugaro^{1,2}, A. I. Karakas³, and C. Iliadis⁴

¹ Sterrekundig Instituut, University of Utrecht, Postbus 80000 3508 TA Utrecht, The Netherlands
e-mail: m.a.vanraai@phys.uu.nl, m.lugaro@phys.uu.nl

² Centre for Stellar and Planetary Astrophysics, School of Mathematical Sciences, Monash University, Victoria 3800, Australia

³ Research School of Astronomy and Astrophysics, Mt. Stromlo Observatory, Cotter Rd., Weston, ACT 2611, Australia
e-mail: akarakas@mso.anu.edu.au

⁴ Department of Physics and Astronomy, University of North Carolina, Chapel Hill, NC 27599-3255, USA; Triangle Universities Nuclear Laboratory, P. O. Box 90308, Durham, NC 27708-0308, USA
e-mail: iliadis@unc.edu

Received / Accepted

ABSTRACT

Context. Stardust is a class of presolar grains each of which presents an ideally uncontaminated stellar sample. Mainstream silicon carbide (SiC) stardust formed in the extended envelopes of carbon-rich asymptotic giant branch (AGB) stars and incorporated the radioactive nucleus ^{26}Al as a trace element.

Aims. The aim of this paper is to analyse in detail the effect of nuclear uncertainties, in particular the large uncertainties of up to four orders of magnitude related to the $^{26}\text{Al}_g(p, \gamma)^{27}\text{Si}$ reaction rate, on the production of ^{26}Al in AGB stars and compare model predictions to data obtained from laboratory analysis of SiC stardust grains. Stellar uncertainties are also briefly discussed.

Methods. We use a detailed nucleosynthesis postprocessing code to calculate the $^{26}\text{Al}/^{27}\text{Al}$ ratios at the surface of AGB stars of different masses ($M = 1.75, 3, \text{ and } 5 M_{\odot}$) and metallicities ($Z = 0.02, 0.012, \text{ and } 0.008$).

Results. For the lower limit and recommended value of the $^{26}\text{Al}_g(p, \gamma)^{27}\text{Si}$ reaction rate, the predicted $^{26}\text{Al}/^{27}\text{Al}$ ratios replicate the upper values of the range of the $^{26}\text{Al}/^{27}\text{Al}$ ratios measured in SiC grains. For the upper limit of the $^{26}\text{Al}_g(p, \gamma)^{27}\text{Si}$ reaction rate, instead, the predicted $^{26}\text{Al}/^{27}\text{Al}$ ratios are ≈ 100 times lower and lie below the range observed in SiC grains. When considering models of different masses and metallicities, the spread of more than an order of magnitude in the $^{26}\text{Al}/^{27}\text{Al}$ ratios measured in stellar SiC grains is not reproduced.

Conclusions. We propose two scenarios to explain the spread of the $^{26}\text{Al}/^{27}\text{Al}$ ratios observed in mainstream SiC, depending on the choice of the $^{26}\text{Al}_g+p$ reaction rate. One involves different times of stardust formation, the other involves extra-mixing processes. Stronger conclusions on the interpretation of the Al composition of AGB stardust will be possible after more information is available from future nuclear experiments on the $^{26}\text{Al}_g+p$ reaction.

Key words. nuclear reactions, nucleosynthesis, abundances – stars: AGB and post-AGB

1. Introduction

Meteoritic stellar grains are solid samples of stars that can be studied in terrestrial laboratories. Condensed in the cooling gas outflows from ancient stars, they became part of the interstellar medium from which the Solar System formed some 4.6 billion years ago. Because they were encapsulated in primitive meteorites they remained ideally uncontaminated by Solar System material. The highly unusual isotopic ratios, with respect to solar, found in these “stardust” grains indicate that they are of stellar origin and can therefore be used as a diagnostic tool for verifying predictions from models of stellar evolution and nucleosynthesis (cf. Anders & Zinner 1993; Zinner 1998; Clayton & Nittler 2004; Lugaro 2005). Stardust grains come in many mineralogical flavours but of particular interest in this work are silicon carbide (SiC) grains.

“Mainstream” SiC grains (>90% of stellar SiC grains) contain isotopic abundances of heavy elements characteristic of the *slow* neutron capture process (the *s* process) and are thus believed to have originated from asymptotic giant branch (AGB) stars (Lugaro et al. 1999, 2003a), which show enrichments at their surface of *s*-process elements such as Zr, Ba, and even the unstable Tc (Merill 1952; Smith & Lambert 1990; Busso et al.

2001). These stars are evolved giants in the final nuclear burning stage of evolution (see Herwig 2005, for a recent review). Briefly, the AGB phase is important because of the occurrence of instabilities of the He-burning shell, known as thermal pulses (TPs). Inbetween TPs the H-shell provides most of the stellar luminosity. After the occurrence of a thermal pulse the third dredge-up (TDU) may occur, where the products of the partial He-burning such as ^{12}C , along with other nucleosynthetic products such as *s*-process elements, are mixed to the stellar surface.

An interesting nucleosynthetic product of AGB stars is the radioactive isotope ^{26}Al ($T_{1/2} = 0.717$ Myr). ^{26}Al is produced by proton captures on ^{25}Mg during H burning, when it can also be consumed by proton captures, depending on the rate of the $^{26}\text{Al}+p$ reaction, and destroyed by neutron captures in the thermal pulse because of the relatively high $^{26}\text{Al}(n,p)^{26}\text{Mg}$ and $^{26}\text{Al}(n,\alpha)^{23}\text{Na}$ rates. Neutrons in the TP are provided by the $^{22}\text{Ne}(\alpha,n)^{25}\text{Mg}$ reaction if the temperature exceeds ≈ 300 million K. When the TDU occurs the ^{26}Al in the thin top layer of the intershell region not involved in the convective pulse, together with the ^{26}Al that survived neutron captures in the TP, is carried to the surface. For a detailed description of the nucleosynthesis of ^{26}Al in AGB stars see Mowlavi & Meynet (2000). The combination of nucleosynthesis in the intershell and the occurrence of

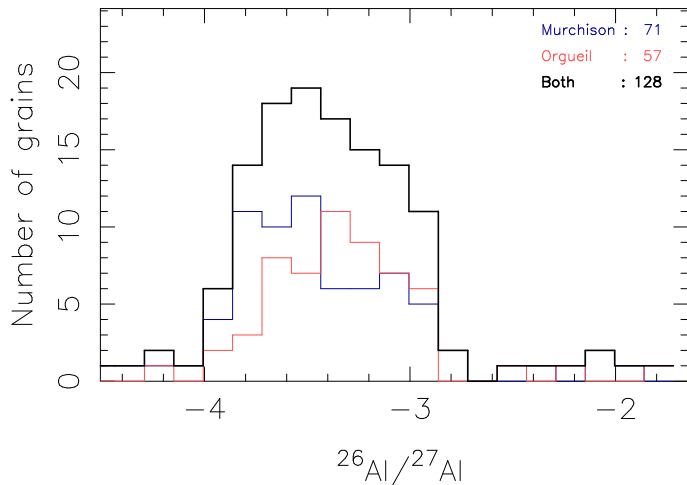


Fig. 1. Histogram of binned $^{26}\text{Al}/^{27}\text{Al}$ ratios measured in mainstream SiC stardust grains found in the Murchison and Orgueil meteorites. The total number of grains for which the $^{26}\text{Al}/^{27}\text{Al}$ ratios were measured is indicated in the upper right hand corner.

the TDU allows AGB stars of masses roughly between $1.5 M_{\odot}$ and $4 M_{\odot}$ to eventually become carbon rich (Groenewegen et al. 1995), which is a necessary condition for the formation of SiC grains. Al is incorporated in SiC grains as a trace element.

Since the abundance of Mg in SiC grains is much lower than that of Al, excesses in ^{26}Mg , together with solar $^{25}\text{Mg}/^{24}\text{Mg}$ ratios, observed in meteoritic stardust SiC grains are a measure of the ^{26}Al abundance at the time and place of formation of the grain. Note that if spallation reactions on the grains during their residence time in the interstellar medium had been responsible for the observed huge excesses in ^{26}Mg , this would also result in variations of the $^{25}\text{Mg}/^{24}\text{Mg}$ ratios, which are not observed. The distribution of the available $^{26}\text{Al}/^{27}\text{Al}$ data for mainstream SiC grains (Hoppe et al. 1994; Huss et al. 1997) is presented in Fig. 1. The majority of the grains are distributed between ratios of $\approx 10^{-4}$ to 2×10^{-3} . The $^{26}\text{Al}/^{27}\text{Al}$ ratio has also recently been measured in a few SiC grains of the rare type Z, which are believed to have originated in low-Z AGB stars (Zinner et al. 2007). The data points cover the same spread as the mainstream grains and low metallicity AGB models give similar results to our \approx solar metallicity models. Hence, our discussion can be applied to Z grains as well.

The aim of this paper is to analyse in detail the effect of the uncertainty in the $^{25}\text{Mg}(p, \gamma)^{26}\text{Al}$ and $^{26}\text{Al}_g(p, \gamma)^{27}\text{Si}$ reaction rates on the production of ^{26}Al in carbon rich AGB stars and compare the model predictions to the data obtained from mainstream SiC grains. While the $^{25}\text{Mg}+p$ is uncertain by a factor of ≈ 2 at the temperature of interest for H burning during the AGB stage (≈ 60 million K), the $^{26}\text{Al}+p$ reaction rate is uncertain by four orders of magnitude (see Fig. 2) due to possible contributions from as yet unobserved low-energy resonances (Iliadis et al. 2001; Angulo et al. 1999). We evaluate the effect of such huge uncertainties on the outputs of AGB models and see if any constraints can be derived from comparison of these models to the SiC data. Stellar model uncertainties will also be briefly discussed.

The study of radioactive isotopes in stardust grains is of interest also because they represent clocks to measure the timescale for the formation of dust around AGB stars (Zinner et al. 2006a; Davis & Gallino 2006). It is still very difficult to pin down the exact mechanism by which dust is formed

around AGB stars, see for example discussion in Nuth et al. (2006), and any insight on the timescale of grain formation therefore represents a useful constraint.

We also note that ^{26}Al is produced by proton captures at the base of the envelope (hot bottom burning, HBB) in intermediate mass AGB stars ($M \gtrsim 5 M_{\odot}$) and in AGB stars of lower masses if extra mixing is invoked, which is usually done to explain the composition of a particular fraction of stardust oxide grains showing a strong depletion of ^{18}O along with high ^{26}Al (Nittler et al. 1997; Nollett et al. 2003). Here we present only one model of an intermediate mass AGB star because they are not main producers of SiC stardust. In fact, HBB prevents massive, metal-rich ($Z > 0.004$) AGB stars from developing a carbon rich envelope by converting C into N. Moreover, the isotopic signatures of C, N, Si, and heavy elements in mainstream SiC grains cannot be reconciled with massive AGB parent stars (Lugaro et al. 1999, 2003a). For example, HBB produces $^{12}\text{C}/^{13}\text{C}$ in the range 3 to 10, while the mainstream SiC range is 20 to 100 and high neutron densities in the thermal pulses produce enhancements in the neutron-rich isotope ^{96}Zr , which is instead observed to be depleted in mainstream SiC grains. We have not included extra mixing in our models, but will discuss its possible implications in §4, based on the models of Nollett et al. (2003). In §2 we present the details of the methods and models we have used. In §3 we show the results we obtained, which we discuss in §4. We conclude with §5 where we present a summary and our main conclusions.

2. Methods and Models

2.1. Evolutionary and Nucleosynthesis codes

We calculate the nucleosynthesis with a detailed post-processing code for which the stellar structure inputs were calculated beforehand. The stellar structure program we use has a small network of 6 species: H, ^3He , ^4He , C, N, and O (see e.g. Lattanzio 1986), involved in the main energy generation. To compute abundances of more species we use a post-processing code. The code is described in detail in Lattanzio et al. (1996). Briefly: we input the structure (e.g. temperature, density, details of the convective regions, position of the H and He-burning shells as a function of interior mass and time) from the stellar evolution code to compute the abundances of species not involved in energy generating reactions. The post-processing step computes its own mass mesh with sufficient resolution in each burning shell (around 25 mass shells) to adequately resolve changes in abundances owing to nuclear burning. Because we assume the structure is fixed in the post-processing step we assume that the extra species and reaction rates added do not change the structure. For this reason we concentrate on uncertainties for reactions that produce negligible energy, such as those involved in the NeNa and MgAl chains, and neutron capture reactions. The details of the nucleosynthesis network are outlined in Lugaro et al. (2004), however, we remind the reader that we include 59 light nuclei and 14 iron-group species. We also add the fictional particle g to count the number of neutron captures occurring beyond ^{62}Ni (Lattanzio et al. 1996; Lugaro et al. 2004) in a similar manner to Jorissen & Arnould (1989).

The bulk of our 527 reaction rates are from the REACLIB tables (Thielemann et al. 1986) updated as described in Lugaro et al. (2004) and Karakas et al. (2006).

In our calculations we used models of $1.75 M_{\odot}$ with a metallicity (Z) of 0.008, of $3 M_{\odot}$ with $Z = 0.02, 0.012$, and 0.008 and of $5 M_{\odot}$ with $Z = 0.02$ and the mass loss pre-

scription from Vassiliadis & Wood (1993). The $1.75 M_{\odot}$ and $3 M_{\odot}$ models produce a carbon over oxygen ratio in excess of unity. More information on these stellar models can be found in Lugaro et al. (2003b), Karakas et al. (2006), and Karakas et al. (2007). Models of low-mass AGB stars of approximately solar metallicity are shown to be the best to reproduce various features of stardust mainstream SiC grains: from the He and Ne composition (Gallino et al. 1990), to the $^{12}\text{C}/^{13}\text{C}$ ratios, which are the same as observed in Galactic C stars with metallicity close to solar (Hoppe & Ott 1997), to the heavy element compositions (Lugaro et al. 2003a). Consequently, we focus on our AGB models of low mass and Z close to solar that become carbon rich. The initial abundances we use were taken from Anders & Grevesse (1989) for $Z = 0.02$ and we assume scaled solar for the $Z = 0.008$ models. The $Z = 0.012$ models are based on the Asplund et al. (2005) and Lodders (2003) solar abundance table which prescribes a solar metallicity of $Z = 0.012$.

2.2. The reaction rates

The rates of interest are those of the $^{25}\text{Mg}(p, \gamma)^{26}\text{Al}_g$, $^{25}\text{Mg}(p, \gamma)^{26}\text{Al}_m$, and $^{26}\text{Al}_g(p, \gamma)^{27}\text{Al}$ reactions. $^{26}\text{Al}_g$ is the ground state of ^{26}Al , whereas $^{26}\text{Al}_m$ is the metastable state with a half life of 6.3452 s. Since the metastable state of ^{26}Al is very short lived, the $^{25}\text{Mg}(p, \gamma)^{26}\text{Al}_m$ rate results in the production of essentially no ^{26}Al , but rather ^{26}Mg . Whenever we use ^{26}Al with no subscript we mean the total sum of the metastable and ground state of ^{26}Al . In practice this means $^{26}\text{Al}_g$, because the isomeric state is very unstable. The rates were taken from Iliadis et al. (2001). We calculated models using all the nine combinations of the lower limits (LL), recommended values (RC), and upper limits (UL) of the rates, where the rate errors of the reactions $^{25}\text{Mg}(p, \gamma)^{26}\text{Al}_g$ and $^{25}\text{Mg}(p, \gamma)^{26}\text{Al}_m$ are correlated. This assumption is justified since the uncertainties arise from the entrance channel partial width which is common to both interactions. The bulk of the rates in our code are calculated using fits in the 7-coefficient format of REACLIB; the rates of interest were read directly from the tabulated rates.

Figure 2 shows the LL, RC, and UL rates for the $^{25}\text{Mg}(p, \gamma)^{26}\text{Al}_g$ and $^{26}\text{Al}_g(p, \gamma)^{27}\text{Al}$ reactions for the temperature range dominant in the H burning shell during the AGB phase, where 6×10^7 K is approximately the peak temperature for all of the used models, except the one with $5 M_{\odot}$ and $Z = 0.02$ where it is 8×10^7 K. The upper limit of the $^{26}\text{Al}_g(p, \gamma)^{27}\text{Al}$ rate is up to four orders of magnitude higher than the lower limit and results, as shown below, in a two orders of magnitude lower abundance of ^{26}Al . These large uncertainties arise from as yet undetected low-energy resonances. In particular, an expected resonance at a center-of-mass energy of 94 keV, with a predicted upper limit of its strength of $\omega\gamma < 10^{-8}$ eV, seems to play the most important role.

3. Results

Figure 3 shows our predictions for the $^{26}\text{Al}/^{27}\text{Al}$ ratio at the surface of the star as a function of C/O for the $3 M_{\odot}$ $Z=0.02$ model and all nine different combinations of the LL, RC, and UL of the rates. All the lines show a very similar trend: the $^{26}\text{Al}/^{27}\text{Al}$ ratio increases sharply with the first few TDUs and then becomes approximately constant. This is because during the first few TPs the mass fraction of ^{26}Al dredged up to the surface is 6.2×10^{-5} in the small region ($\approx 10^{-4} M_{\odot}$) of the H-burning ashes (region A of Mowlavi & Meynet 2000) and $\approx 1.8 \times 10^{-5}$ in the rest of

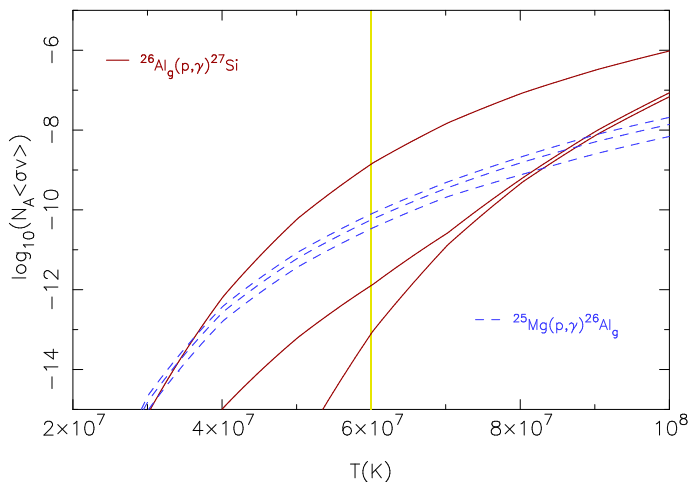


Fig. 2. The lower limit (bottom line), recommended value (middle line), and upper limit (upper line) of the $^{25}\text{Mg}(p, \gamma)^{26}\text{Al}_g$ (dashed lines) and $^{26}\text{Al}_g(p, \gamma)^{27}\text{Al}$ (solid lines) reaction rates. The vertical line denotes the approximate temperature of interest ($T \approx 6 \times 10^7$ K).

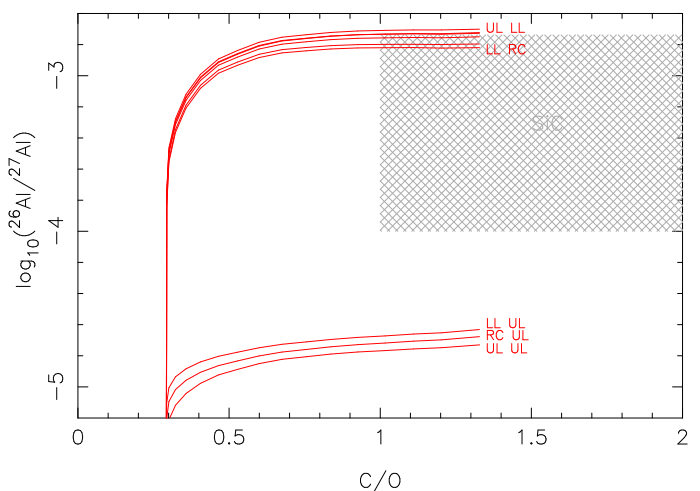


Fig. 3. Surface $^{26}\text{Al}/^{27}\text{Al}$ ratio versus C/O ratios for a star of mass $3 M_{\odot}$, metallicity $Z = 0.02$, and a partial mixing zone (PMZ) of 1×10^{-3} (see §3.1) using all combinations of upper, lower and recommended values for the rates under consideration. At the end of some selected lines a label indicates the values used for the $^{25}\text{Mg}(p, \gamma)^{26}\text{Al}_g$ and $^{26}\text{Al}_g(p, \gamma)^{27}\text{Al}$ rates, in that order, where LL = lower limit, RC = recommended, and UL = upper limit. The grey crosshatched box is a schematic representation of the range of the $^{26}\text{Al}/^{27}\text{Al}$ values observed in stardust mainstream SiC grains (see Fig. 1), which can form only when $\text{C/O} > 1$.

the intershell (region D of Mowlavi & Meynet 2000). (See also Table 2 of Lugaro et al. 2001). However, as the pulse number increases, the temperature at the base of the convective intershell region increases, and the $^{22}\text{Ne}(\alpha, n)^{25}\text{Mg}$ reaction becomes more active, this frees up more neutrons resulting in more ^{26}Al destruction by neutron capture. The abundance of ^{26}Al in the last computed TP is in fact $\approx 2 \times 10^{-8}$ in the intershell. The TDU of this small amount of ^{26}Al is just enough to ensure that the small fraction ($\approx 5\%$) of ^{26}Al at the stellar surface that decays during the interpulse period is replenished. As a result the prediction lines flatten.

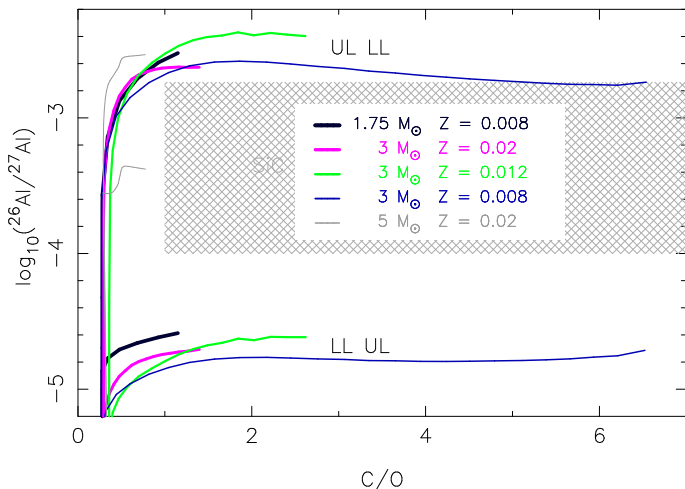


Fig. 4. $^{26}\text{Al}/^{27}\text{Al}$ abundance ratios for models of different mass and metallicity. Two calculations are shown for each model: the top line represents the reaction rate combination: UL LL and the bottom line the reaction rate combination: LL UL (see Fig. 3). The fact that the $3 M_{\odot}$ $Z=0.02$ line is slightly higher than shown in Fig. 3 is due to the fact that a partial mixing zone was included in the calculations shown in Fig. 3, while no partial mixing zone is included in the calculations shown in this figure.

Two main classes of prediction lines can be distinguished:

1. When considering the models computed using the RC and LL values for the $^{26}\text{Al}_g(p, \gamma)^{27}\text{Si}$ rate the variation among these is of a factor of a mere 1.32. Of this, a factor of ≈ 1.26 is derived when varying the $^{25}\text{Mg}(p, \gamma)^{26}\text{Al}_g$ reaction rate between the LL and the UL, while a factor of ≈ 1.05 is derived when varying the $^{26}\text{Al}_g(p, \gamma)^{27}\text{Si}$ reaction rate between the LL and the RC rate. All the lines lie around the upper end of the SiC grain data range.
2. When considering the models computed using the UL values for the $^{26}\text{Al}_g(p, \gamma)^{27}\text{Si}$ rate, the $^{26}\text{Al}/^{27}\text{Al}$ ratio is roughly two orders of magnitude smaller than the ratios computed using the RC and the LL values of the rate, hence falling below the range of values observed in mainstream SiC grains.

In Fig. 4 we present the results for different masses and metallicities. We can see the same behaviour here as described above: the upper limit of the $^{26}\text{Al}_g(p, \gamma)^{27}\text{Si}$ reaction rate always results in a factor of ≈ 100 less ^{26}Al , except for the $5 M_{\odot}$ model, in which case the difference is of a factor of ≈ 10 . Note that the production of ^{26}Al in this massive AGB model is due to the operation of the second and third dredge-up and *not* due to hot bottom burning because the temperature at the bottom of the convective envelope is not high enough to produce ^{26}Al (see discussion in Lugaro et al. 2007). This explains why our detailed model shows a large effect in the ^{26}Al abundance as a result of the uncertainties in the $^{26}\text{Al}_g(p, \gamma)^{27}\text{Si}$ reaction rate, while the synthetic models of Izzard et al. (2007), which only describe the effect of hot bottom burning, do not show this effect.

All the models computed using the RC or LL for the $^{26}\text{Al}_g(p, \gamma)^{27}\text{Si}$ reaction rate produce $^{26}\text{Al}/^{27}\text{Al}$ ratios at the upper end of the observed distribution. Similar results were obtained (for the RC case) by Mowlavi & Meynet (2000) and Zinner et al. (2007) for several models of different masses and Z , and by Cristallo et al. (2006) for a $2 M_{\odot}$ $Z = 0.015$ model.

3.1. Other uncertainties

Some uncertainty is introduced by the neutron capture reaction rates. We use for these rates the estimates of Koehler et al. (1997) and Skelton et al. (1987). These works suggest for the $^{26}\text{Al}_g(n, p)^{26}\text{Mg}$ rate a value similar to that of Caughlan & Fowler (1988), ≈ 250 mbarn (at 23 keV, taken as typical temperature in the thermal pulse) and for the $^{26}\text{Al}_g(n, \alpha)^{23}\text{Na}$ rate a value roughly a factor of two higher than Caughlan & Fowler (1988), ≈ 180 mbarn (at 23 keV). The $^{26}\text{Al}_g(n, \gamma)^{27}\text{Al}$ rate is much smaller than the aforementioned neutron capture channels: ≈ 4.5 mbarn (at 23 keV, Bao et al. 2000). We conservatively estimated the uncertainties of these rates to be of a factor of two both above and below the values we use. When we multiplied the rate of all n -capture rates on ^{26}Al by a factor of two we ended up with half as much ^{26}Al , similarly when we decreased the n -capture rates by a factor of two, we ended up with twice as much ^{26}Al . Overall, the uncertainty is at most of a factor of four.

Since neutrons released by the $^{22}\text{Ne}(\alpha, n)^{25}\text{Mg}$ reaction destroy ^{26}Al , the uncertainty of this reaction rate introduces another uncertainty in the ^{26}Al abundance. Between the lower and upper limit (a range of about a factor of 15, Karakas et al. 2006) of this rate the ^{26}Al abundance varies with a factor of 1.8 for the $3 M_{\odot}$ and $Z = 0.02$ model.

Note that the uncertainties of a factor of ≈ 20 (Iliadis et al. 2001) in the $^{27}\text{Al}+p$ reaction rate do not change the ^{27}Al abundance because this reaction is too slow in the H-burning shell of AGB stars.

As for stellar uncertainties: we artificially included a partial mixing zone in the top layers of the intershell in the way described in detail by Lugaro et al. (2004). There, protons combine with ^{12}C to make ^{13}C , which releases neutrons for the s process via $^{13}\text{C}(\alpha, n)^{16}\text{O}$ during the interpulse periods, however, the nature of the mixing is still debated (Herwig 2005). Varying the size of the ^{13}C pocket from 0 to 2×10^{-3} introduces a spread in the $^{26}\text{Al}/^{27}\text{Al}$ ratio of at most a factor of 1.4. Varying the proton profile in the partial mixing zone changes the relative importance of the ^{14}N -poor and ^{14}N -rich regions of the pocket. As shown in Fig. 1 of Goriely & Mowlavi (2000), in the ^{14}N -poor region ^{26}Al is completely destroyed, while in the ^{14}N -rich region it is destroyed to an abundance of the order of 10^{-7} in number. Thus, changes in the proton profile would not have a significant impact on the overall ^{26}Al abundance in these stars.

Mass loss and third dredge-up are very uncertain physical features of AGB stars. However, we expect that changes in the TDU efficiency, caused by variations in the input physics, and changes of the mass loss values will not affect our results significantly. This is because we are looking at C-rich stars and the $\text{C/O} > 1$ constraint sets the dilution factor in our models to ≈ 1 part of intershell material to ≈ 30 parts of envelope material. This dilution factor would necessarily produce $^{26}\text{Al}/^{27}\text{Al} \approx 10^{-3}$, independently of which TDU efficiency and mass loss rate have been employed to achieve it.

Extra-mixing processes due to rotation or other mechanisms may also be at work in these stars. Extra mixing is the hypothesis that some of the material from the convective envelope is mixed into the radiative layer that resides on top of the hydrogen shell. It is also commonly referred to as: “deep mixing” and “cool bottom processing”. Extra mixing was originally introduced into the first giant phase of evolution to explain several abundance peculiarities, including lower than predicted $^{12}\text{C}/^{13}\text{C}$ ratios in first giant branch stars (see e.g. Sweigart & Mengel 1979). Extra mixing has been invoked for AGB stars to explain the $^{12}\text{C}/^{13}\text{C}$ ratio

in C-rich stars (Abia & Isern 2000), as well as in mainstream and Z SiC grains (Zinner et al. 2006b), the O composition of AGB stars (see e.g. Wasserburg et al. 1995) and the O and Al composition of a fraction of stellar oxide grains (Nollett et al. 2003). The possible effect of extra-mixing on the ^{26}Al abundance will be discussed in §4.2.

4. Discussion

With the exception of the $5 M_{\odot}$ model, the models presented in Fig. 4 should represent the set of stars, in terms of mass and metallicity, responsible for mainstream SiC stardust grains. However, the spread of the $^{26}\text{Al}/^{27}\text{Al}$ SiC grain data is much larger than that of the models. The spread of the data is not an error range, but arises from considering the large number of single grains (128, to be exact, see Fig. 1). The $^{26}\text{Al}/^{27}\text{Al}$ abundance ratios range a factor of ≈ 20 in the data, whereas the models show at best a spread of about a factor of 2. We propose two scenarios to explain the observed range:

4.1. The $^{26}\text{Al}_g+p$ reaction rate corresponds to its current LL or RC value

In this case we need to explain the fact that the data extends below the prediction lines, which may reflect the fact that stardust SiC grains have a long interval of formation time between a time close to when TDU has enriched the stellar winds with ^{26}Al and approximately two million years later. This time delay would allow the decay of ^{26}Al into ^{26}Mg , the latter of which is not incorporated in the grains. Since the mechanism by which the large (up to $25 \mu\text{m}$) stardust SiC grains found in meteorites are formed around single AGB stars is not understood, and in any case it probably does not involve timescales longer than $\sim 10^5$ yr (Nuth et al. 2006), we speculate upon different possibilities.

A long interval of formation time could be achieved if the grains were formed either (i) in the winds of extrinsic carbon stars formed in a binary system (in this case the absence of ^{26}Al would be conceptually equivalent to that of Tc in these stars) or, perhaps, (ii) in a long-lived circumbinary disk that formed after one of the binary stars evolved through the AGB phase. Note that circumbinary disks have already been proposed as the site of origin of at least some meteoritic stardust in order to explain the large observed sizes of the grains $> 0.5 \mu\text{m}$ (Jura 1997). The long timescale of stardust grain formation proposed here is not ruled out by the analysis of radioactive heavy nuclei in mainstream SiC, which have been discussed in detail by Davis & Gallino (2006).

4.2. The $^{26}\text{Al}_g(p, \gamma)^{27}\text{Si}$ reaction rate corresponds to its current UL

In this case we need to explain the fact that the data extends above the prediction lines, which may reflect the occurrence of extra-mixing processes. Extra mixing could produce $^{26}\text{Al}/^{27}\text{Al}$ ratios higher than our predictions and the spread in the data could be achieved by a range of temperatures (i.e. depths) to which the mixed material is exposed. The main problem with invoking extra mixing is that we still miss the physical mechanism behind the process, even if some steps forward in this search have been made recently (Eggleton et al. 2006; Charbonnel & Zahn 2007; Busso et al. 2007).

Note that assuming the UL for the $^{26}\text{Al}_g(p, \gamma)^{27}\text{Si}$ reaction rate does not affect ^{26}Al production in supernovae, since most of

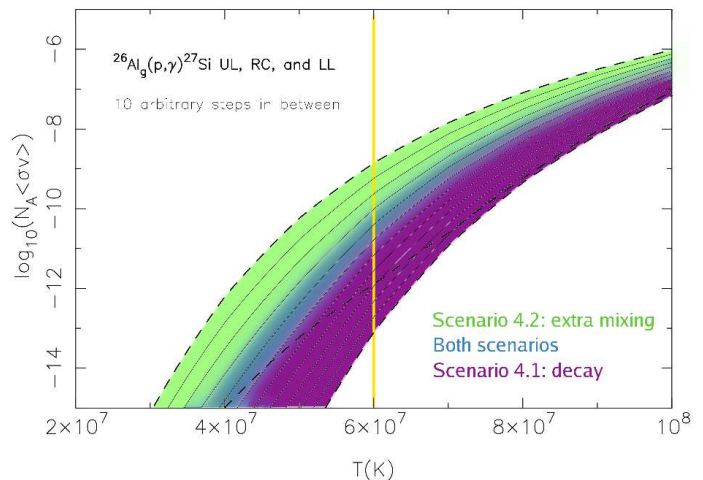


Fig. 5. Upper limit, recommended value, and lower limit of the $^{26}\text{Al}_g(p, \gamma)^{27}\text{Si}$ reaction rate (dashed lines) as in Fig. 2, with 10 logarithmically equidistant steps in between the LL and the UL (solid lines). The shaded areas represent roughly which value of the $^{26}\text{Al}_g(p, \gamma)^{27}\text{Si}$ reaction rate corresponds to which scenario. The vertical yellow line denotes the approximate temperature of interest (as in Fig.2).

this nucleus is produced during the explosion where the main destruction channel for ^{26}Al is neutron capture (Limongi & Chieffi 2006). Thus, the present scenario would not be in contrast with the match to the observed live ^{26}Al in the Galaxy (Diehl 2006). On the other hand, production of ^{26}Al in Wolf-Rayet stars (Arnould et al. 2006) and in intermediate-mass AGB stars by hot bottom burning would be affected (for a detailed analysis on the latter see Izzard et al. 2007). As a consequence, the discussion on the origin of stardust spinel grain OC2 from a massive AGB star (Lugaro et al. 2007) would have to be revised.

5. Summary and conclusions

We have shown that the large uncertainty of the $^{26}\text{Al}_g+p$ reaction rate has important implications when comparing AGB models to the $^{26}\text{Al}/^{27}\text{Al}$ ratios observed in stardust mainstream SiC grains. We have presented two scenarios to explain the observed distribution: one involves using the LL or the RC rate and invoking a relatively long timescale of grain formation, possibly connected to processes occurring in binary systems. The other involves using the UL of the rate and invoking extra-mixing processes.

To check in details which scenario would correspond to which values of the rate we have computed the $^{26}\text{Al}/^{27}\text{Al}$ ratios in the $3 M_{\odot}$, $Z = 0.02$ model for ten different rates calculated as logarithmically equidistant steps in between the LL and UL. The results are shown in Fig. 5. The decay scenario has to be invoked with rate values ranging from the LL up to the 6th intermediate line from below. For rates from roughly the 8th intermediate line up to the UL the $^{26}\text{Al}/^{27}\text{Al}$ ratio lies below the SiC data, and hence would imply the extra mixing scenario.

Our work calls for more laboratory measurements of the $^{26}\text{Al}/^{27}\text{Al}$ ratios in stardust SiC grains of different sizes and for improved measurements of the $^{26}\text{Al}_g+p$ reaction rates. A direct measurement of the 94 keV resonance may prove challenging, considering the difficult preparation of a radioactive ^{26}Al beam-stop target that will not degrade under intense proton bombardment. An interesting attempt at studying the nuclear structure of the corresponding compound level in ^{27}Si by using the

$^{26}\text{Al}_g(^3\text{He},d)^{27}\text{Si}$ reaction has been reported in Vogelaar et al. (1996). Unfortunately, the contamination of their evaporated transmission target precluded the observation of transfers to any threshold states. A remeasurement of the transfer reaction by using an isotopically and elementally pure implanted ^{26}Al target seems more promising.

Once the estimate of the $^{26}\text{Al}_g(p,\gamma)$ reaction is less uncertain, we will be able to readdress the issue of ^{26}Al production in AGB stars and deliver stronger conclusions on the implications for dust formation around AGB stars and extra-mixing processes.

Acknowledgements. ML gratefully acknowledges the support of NWO through the VENI grant. We thank Peter Hoppe and Gary Huss for providing us with the datatables of the grain measurements and for helpful and instructive discussion. We thank Alessandro Chieffi and Marco Limongi for discussion. AIK gratefully acknowledges the financial support of the Australian Research Council from the Discovery Project funding scheme (project number DP0664105). We thank the referee, Marcel Arnould, for a detailed report which helped to improve the paper.

References

- Abia, C., & Isern, J. 2000, *IAUS*, 177, 89A
- Anders, E., & Grevesse, N. 1989, *Geochim. Cosmochim. Acta*, 53, 197
- Anders, E., & Zinner, E. 1993, *Meteoritics*, 28, 490
- Angulo, C., Arnould, M., Rayet, M. et al. 1999, *Nucl. Phys. A*, 656, 3
- Arnould, M., Goriely, S., & Meynet, G. 2006, *A&A*, 453, 653
- Asplund, M., Grevesse, N. & Sauval, A. J. 2005, in *Cosmic Abundances as Records of Stellar Evolution and Nucleosynthesis in honor of David L. Lambert*, eds. T. G. Barnes III, & F. N. Bash (San Francisco: Astronomical Society of the Pacific) 336, 25
- Bao, Z. Y., Beer, H., Käppeler, F. et al. 2000, *Atomic Data and Nuclear Data Tables*, 76, 70
- Busso, M., Gallino, R., & Wasserburg, G. J. 1999, *ARA&A*, 37, 239
- Busso, M., Gallino, R., Lambert, D. L., Travaglio, C., & Smith, V. V. 2001, *ApJ*, 557, 802
- Busso, M., Wasserburg, G. J., Nollett, K. M., & Calandra, A. 2007, *ApJ*, accepted astro-ph:0708.2949
- Cannon, R.C. 1993, *MNRAS*, 263, 817
- Caughlan, G.R., & Fowler, W.A. 1988, *Atom. Data Nucl. Data Tables*, 40, 283
- Charbonnel, C., & Zahn, J.-P. 1007, *A&A*, in press [astro-ph/0703302]
- Clayton, D. D., & Nittler, L. R. 2004, *ARA&A*, 42, 39
- Cristallo, S., Gallino, R., Straniero, O., Piersanti, L., & Domínguez, I. 2006, *MemSAIt*, 77, 774
- Davis, A. M., & Gallino, R. 2006, *MemSAIt*, 77, 885
- Diehl, R. 2006, *New Astronomy Reviews*, 50, 534
- Eggleton, P. P., Dearborn, D. S. P., & Lattanzio, J.C. 2006, *Science*, 314, 1580
- Frost, C. A., & Lattanzio, J. C. 1996, *ApJ*, 473, 383
- Gallino, R., Busso, M., Picchio, G., & Raiteri, C. M. 1990, *Nature* 348, 298
- Groenewegen, M. A. T., van den Hoek, L. B., & de Jong, T. 1995, *A&A*, 293, 381
- Goriely, S. & Mowlavi, N. 2000, *A&A*, 362, 599
- Herwig, F. 2005, *ARA&A*, 43, 435
- Hoppe, P., Amari, S., Zinner, E., Ireland, T., & Lewis, R. S. 1994, *ApJ*, 430, 870
- Hoppe, P., & Ott, U. 1997, in “Astrophysical Implications of the Laboratory Study of Presolar Materials”, ed. Thomas J. Bernatowicz & Ernst Zinner, American Institute of Physics Conference proceedings 402, 27
- Hoppe, P., Strebler, R., Eberhardt, P., Amari, S., & Lewis, R.S. 1996, *Geochim. Cosmochim. Acta*, 60, 883
- Huss, G.R., Hutcheon, I.D., & G. J. Wasserburg, G. J. 1997, *Geochim. Cosmochim. Acta*, 61, 5117
- Iliadis, C., D’Auria, J. M., Starrfield, S., Thompson, W. J., & Wiescher, M. 2001, *ApJS*, 134, 151
- Izzard, R. G., Lugaro, M., Karakas, A. I., Iliadis, C., & van Raai, M. 2007, *A&A*, 466, 641
- Jorissen A., & Arnould, M. 1989, *A&A*, 221, 161
- Jura, M. 1997, in “Astrophysical Implications of the Laboratory Study of Presolar Materials”, ed. Thomas J. Bernatowicz & Ernst Zinner, American Institute of Physics Conference proceedings 402, 379
- Karakas, A. I., Lugaro, M., & Gallino, R. 2007, *ApJL*, 656, 73
- Karakas, A. I., Lugaro, M., Wiescher, M., Goerres, J., & Ugalde, C. 2006, *ApJ*, 643, 471
- Koehler, P.E., Kavanagh, R.W., & Vogelaar, R.B. et al. 1997, *Phys. Rev. C*, 56, 1138
- Lattanzio, J. 1986, *ApJ*, 311, 708
- Lattanzio, J., Frost, C., Cannon, R., & Wood, P.R. 1996, *Memorie della Societa Astronomia Italiana*, 67, 729
- Limongi, M., & Chieffi, A. 2006, *ApJ*, 647, 483
- Lodders, K. 2003, *ApJ*, 591, 1220
- Lugaro, M. 2005, *Stardust from Meteorites: An Introduction to Presolar Grains, Series in Astronomy and Astrophysics, Vol. 9* (World Scientific, Singapore)
- Lugaro, M., Karakas, A., Champagne, A., Lattanzio J., & Cannon, R. 2001, *MemSAIt*, 72, 319
- Lugaro, M., Karakas, A. I., Nittler, L. R. et al. 2007, *A&A*, 461, 657
- Lugaro, M., Davis, A. M., Gallino, R. et al. 2003a, *ApJ*, 593, 486
- Lugaro, M., Herwig, F., Lattanzio, J. C., Gallino, R., & Straniero, O. 2003b, *ApJ*, 586, 1305
- Lugaro, M., Ugalde, C., Karakas, A. I. et al. 2004b, *ApJ*, 615, 934
- Lugaro, M., Zinner, E., Gallino, R., & Amari, S. 1999, *ApJ*, 527, 369
- Merrill, P. W. 1952, *Science*, 115, 484
- Mowlavi, N., & Meynet, G. 2000, *A&A*, 361, 959
- Nittler, L. R., Alexander, C. M.O’D., Gao, X., Walker, R. M., & Zinner, E. 1997, *ApJ*, 483, 475
- Nollett, K. M., Busso, M., & Wasserburg, G. J. 2003, *ApJ*, 582, 1036
- Nuth, J. A., III, Wilkinson, G. M., Johnson, N. M., & Dwyer, M. 2006, *ApJ*, 644, 1164
- Palacios, A., Charbonnel, C., Talon, S., & Siess, L. 2006, *A&A*, 453, 261
- Skelton, R.T., Kavanagh, R.W., & Sargood, D.G. 1987, *Phys. Rev. C*, 35, 45
- Smith, V. V., & Lambert, D. L. 1990, *ApJS*, 72, 387
- Sweigart, A. V., & Mengel, J. G. 1979, *ApJ*, 229, 624
- Thielemann, F.-K., Arnould, M., & Truran, J.W. 1986, in “Advances in Nuclear Astrophysics”, eds. E. Vangioni-Flam et al., (Gif-sur-Yvette: Editions Frontières), 525
- Vassiliadis, C., & Wood, P.R. 1993, *ApJ*, 413, 641
- Vogelaar, R. B., Mitchell, L. W., Kavanagh, R. W. et al. 1996, *Phys. Rev. C*, 53, 1945
- Wasserburg, G. J., Boothroyd, A. I., & Sackmann, I.-J. 1995, *ApJL*, 447, 37
- Zinner, E. 1998, *Annu. Rev. Earth Planet. Sci.*, 26, 147
- Zinner, E., Amari, S., Guinness, R. et al. 2007, *Geochim. Cosmochim. Acta*, accepted
- Zinner, E., Nittler, L. R., Alexander, C. M. O.’D., & Gallino, R. 2006a, *New Astronomy Reviews*, 50, 574
- Zinner, E., Nittler, L. R., Gallino, R. et al., 2006b, *ApJ*, 650, 350